Redox variations in Mauna Kea lavas, the oxygen fugacity of the Hawaiian plume, and the role of volcanic gases in Earth's oxygenation

Maryjo Brounce[a,1,2], Edward Stolper[a], and John Eiler[a]

[a]Division of Geological and Planetary Sciences, California Institute of Technology, Pasadena, CA 91125

Edited by Donald J. DePaolo, Lawrence Berkeley National Laboratory, Berkeley, CA, and approved July 7, 2017 (received for review November 28, 2016)

The behavior of C, H, and S in the solid Earth depends on their oxidation states, which are related to oxygen fugacity (fO_2). Volcanic degassing is a source of these elements to Earth's surface; therefore, variations in mantle fO_2 may influence the fO_2 at Earth's surface. However, degassing can impact magmatic fO_2 before or during eruption, potentially obscuring relationships between the fO_2 of the solid Earth and of emitted gases and their impact on surface fO_2. We show that low-pressure degassing resulted in reduction of the fO_2 of Mauna Kea magmas by more than an order of magnitude. The least degassed magmas from Mauna Kea are more oxidized than midocean ridge basalt (MORB) magmas, suggesting that the upper mantle sources of Hawaiian magmas have higher fO_2 than MORB sources. One explanation for this difference is recycling of material from the oxidized surface to the deep mantle, which is then returned to the surface as a component of buoyant plumes. It has been proposed that a decreasing pressure of volcanic eruptions led to the oxygenation of the atmosphere. Extension of our findings via modeling of degassing trends suggests that a decrease in eruption pressure would not produce this effect. If degassing of basalts were responsible for the rise in oxygen, it requires that Archean magmas had at least two orders of magnitude lower fO_2 than modern magmas. Estimates of fO_2 of Archean magmas are not this low, arguing for alternative explanations for the oxygenation of the atmosphere.

ocean island basalts | oxygen fugacity | Hawaii volcanism | volcanic degassing | Great Oxidation Event

Modern arc and back-arc basin magmas have higher ratios of Fe^{3+} to total Fe (i.e., $Fe^{3+}/[Fe^{3+}+Fe^{2+}]$, or $Fe^{3+}/\Sigma Fe$), and S^{6+} to total S (i.e., $S^{6+}/[S^{6+}+S^{2-}]$, or $S^{6+}/\Sigma S$), than midocean ridge basalt (MORB) magmas (1–7). Based on the known relationships between $Fe^{3+}/\Sigma Fe$, $S^{6+}/\Sigma S$, oxygen fugacity (fO_2), and melt composition (8, 9) and on recent observations that $Fe^{3+}/\Sigma Fe$ of subduction-related magmas are only weakly dependent on factors such as crystal–liquid fractionation and degassing (7, 10, 11), the higher $Fe^{3+}/\Sigma Fe$ ratios of arc and back-arc basalts relative to MORBs have been attributed by most authors to elevated fO_2 in their mantle sources resulting from addition of oxidized hydrous fluids or silicate melts from subducted slabs (7, 11, 12). Ocean island basalts (OIBs) are more variable in fO_2, with $Fe^{3+}/\Sigma Fe$ and $S^{6+}/\Sigma S$ ratios that range from lower than to higher than MORBs (4, 13–17), but it is unclear whether these differences relate to variable amounts of ancient, more oxidized subducted material in the mantle sources of OIB (e.g., ref. 18) or to other factors related to differences in the petrogenesis of OIB and MORB magmas [e.g., temperature and pressure of melting (15), degassing of certain volatile elements (16, 17)].

There are several processes by which $Fe^{3+}/\Sigma Fe$ and $S^{6+}/\Sigma S$ ratios could change during magmatic differentiation, and these could contribute to the observed variability in fO_2 among basalts erupted at Earth's surface. One possibility is crystal–liquid fractionation: In a system closed to oxygen, olivine and pyroxene crystallization would result in an increase in the $Fe^{3+}/\Sigma Fe$ of residual liquids; alternatively, spinel crystallization could decrease this ratio in residual liquids. Degassing is another possibility: Degassing and loss of H_2 can lead to oxidation of residual liquids (19). Likewise, although CO_3^{2-} species are thought to be the dominant forms of dissolved C in terrestrial magmas, CO is a nonnegligible component of exsolved gases and degassing, and loss of CO-bearing vapor could lead to oxidation of residual liquids (20). Also, both oxidized and reduced forms of S are dissolved in basaltic melts and coexisting gas. Progressive degassing could lead to either oxidation or reduction of the residual melt phase, depending on the speciation of S in the melt and gas. Because the direction of this latter effect has been thought to be pressure-dependent, it has been proposed that the rise of atmospheric oxygen near the Archean–Proterozoic boundary reflected the generation of subaerial crust and a subsequent, progressive decrease in the pressure at which magmas erupted, resulting in an increase in average oxidation state of degassed volcanic volatiles (21, 22).

To isolate and quantify the effects of degassing on the fO_2 of magmas and to place quantitative constraints on the ability of the solid Earth's fO_2 to impact pO_2 at Earth's surface via magmatic degassing, we measured both $Fe^{3+}/\Sigma Fe$ and $S^{6+}/\Sigma S$ ratios in submarine glasses from the Mauna Kea volcano in Hawaii that record shallow degassing of an $S+H_2O+CO_2$-bearing gas phase. These samples are from a well-characterized sample suite recovered by the Hawaii Scientific Drilling Project (HSDP) (23) that records the transition from submarine to subaerial eruption during the shield-building phase of Mauna Kea's growth. In this closely related suite of samples, the concentrations of volatiles are known to vary primarily due to shallow-level degassing, with slight variations in the major element composition that suggest only a small amount of concomitant crystal–liquid fractionation (24). For this suite of OIB

Significance

Volcanic degassing at Mauna Kea volcanoes decreases the oxidation state of both Fe and S in the magmas, consistent with recent results from Kilauea volcano. The least degassed magmas from Mauna Kea are more oxidized than midocean ridge basalt magmas, possibly due to plate tectonic cycling of material from the oxidized surface to the deep mantle, which is then returned to the surface as a component of buoyant plumes. If the degassing trend observed for Mauna Kea applies to basaltic systems more broadly, decompression does not lead to significant changes in the reducing capacity of the exsolved gases and thus cannot explain the rise of oxygen at the Archean/Proterozoic boundary.

Author contributions: M.B., E.S., and J.E. designed research; M.B. performed research; M.B. contributed new reagents/analytic tools; M.B., E.S., and J.E. analyzed data; and M.B., E.S., and J.E. wrote the paper.

The authors declare no conflict of interest.

This article is a PNAS Direct Submission.

[1]Present address: Department of Earth Sciences, University of California, Riverside, CA 92521.

[2]To whom correspondence should be addressed. Email: mbrounce@ucr.edu.

This article contains supporting information online at www.pnas.org/lookup/suppl/doi:10.1073/pnas.1619527114/-/DCSupplemental.

glasses, it is reasonable to attribute observed correlations of volatile contents of glasses with their $Fe^{3+}/\Sigma Fe$ and $S^{6+}/\Sigma S$ ratios nearly entirely to the effects of shallow-level degassing on the valence states of dissolved Fe and S in the liquid, and thereby to the effects of degassing on fO_2.

Materials and Methods

The HSDP recovered >3,000 m of core, most of which samples 150,000- to >500,000-y-old subaerial and submarine basalts from Mauna Kea volcano (25, 26). The glasses range from undegassed to degassed with respect to H_2O and S, although even the so-called undegassed samples likely also lost significant CO_2 during ascent (24). The low-SiO_2 glasses have, on average, higher H_2O contents than high-SiO_2 glasses, but the total S contents of the two suites are similar (Fig. 1 *A*–*D* and ref. 24).

We focused on glassy samples from two intervals of the HSDP2 core drilled in 1999 (23). The first suite consists of high-SiO_2 pillow-rim glasses recovered from 2,703 to 2,841 m below sea level (mbsl), and the second suite consists of low-SiO_2 pillow-rim glasses recovered from 2,438 to 2,470 mbsl. The difference in SiO_2 contents between the two suites is thought to arise as the result of differences in the pressure of melt segregation in the mantle source of Mauna Kea magmas [low-SiO_2 lavas segregate at higher pressures (27)] and/or differences in the extent of melt–rock interaction before or during melt segregation [low-SiO_2 lavas reflect lower extents of melt–rock interaction (26)]. The H_2O and S contents are positively correlated in both suites, and the samples have variable but generally low CO_2 contents (0.16 wt% to 0.81 wt% H_2O; 350 ppm to 1,440 ppm S; 30 ppm to 189 ppm CO_2; see *SI Appendix*). The FeO* (total Fe, expressed as FeO) concentrations of both suites span a narrow range (10.2 wt% to 12.4 wt%; *SI Appendix*, Fig. S6) and do not correlate with S contents, but instead plot below the empirical trend in Fe vs. S contents of basaltic magmas of comparable major element compositions at sulfide saturation (*SI Appendix*, Fig. S6 and ref. 24). Based on these observations, the volatile contents of these submarine glasses have been inferred to reflect variable extents of degassing of $S+H_2O+CO_2$-bearing vapor from magmas that were shallowly stored below the seafloor (5 bars to 50 bars total pressure; *SI Appendix*, Fig. S6 and ref. 24) and then erupted on the seafloor.

To determine the effect of degassing on magmatic fO_2, we measured $Fe^{3+}/\Sigma Fe$ and $S^{6+}/\Sigma S$ ratios of these pillow glasses by micro-X-ray absorption near-edge structure (μ-XANES) spectroscopy (see *SI Appendix* for a description of analytical methods, spectral fitting procedures, and error assessments for both Fe and S; see Dataset S1 for results).

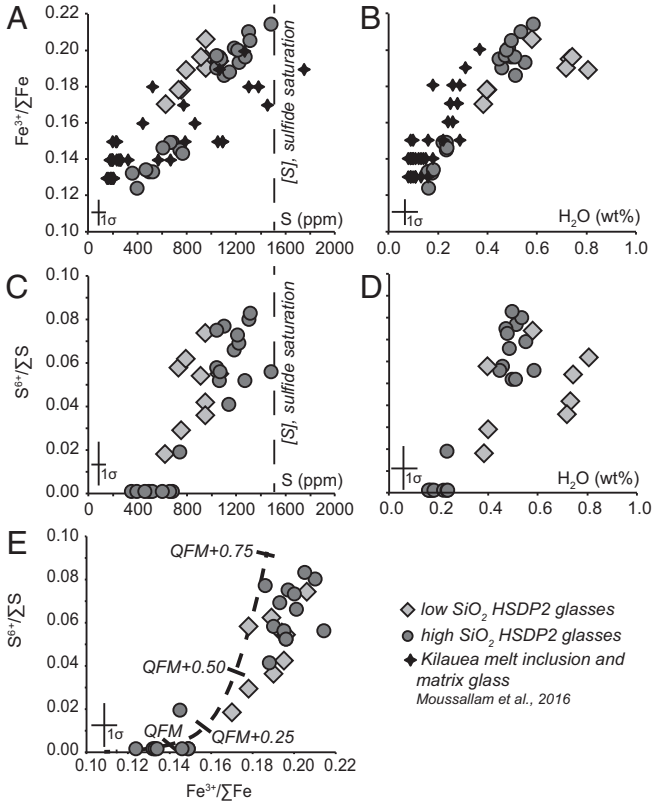

Fig. 1. Observations of the redox states of Fe and S in Hawaiian submarine volcanic glasses from XANES compared with H_2O and S abundances. (*A*) $Fe^{3+}/\Sigma Fe$ ratios v. S concentrations, (*B*) $Fe^{3+}/\Sigma Fe$ ratios v. H_2O concentrations, (*C*) $S^{6+}/\Sigma S$ ratios v. S concentrations, (*D*) $S^{6+}/\Sigma S$ ratios v. H_2O concentrations, and (*E*) $S^{6+}/\Sigma S$ ratios v. $Fe^{3+}/\Sigma Fe$ ratios in the glasses. Representative error bars for each axis are shown in each panel (see *SI Appendix*). Sulfur and H_2O abundance data are from ref. 24. The vertical dashed lines in *A* and *C* are the approximate S content at sulfide saturation for HSDP2 glasses with the highest FeO* content (~12.5 wt%), taken from a line of best fit through S versus FeO* contents of MORB that are sulfide saturated (20, 24). Measurements of $S^{6+}/\Sigma S = 0$ in *A*, *C*, and *E* reflect analyses that lack spectral evidence for S^{6+}, i.e., S^{6+} is below the analytical detection limit. The black dashed curve in *E* shows the calculated trend of $Fe^{3+}/\Sigma Fe$ vs. $S^{6+}/\Sigma S$ ratios for a representative HSDP2 glass as fO_2 is varied. The initial fO_2 is based on the $Fe^{3+}/\Sigma Fe$ ratio and major element glass composition of glass sample SR0915-0.4 (26), at 1,200 °C and 1 atm using the calibration of ref. 8. The corresponding $S^{6+}/\Sigma S$ ratio was then calculated from fO_2 using the calibration of ref. 9. Tick marks show the calculated fO_2 relative to the QFM buffer at 1,200 °C and 1 atm. Data from ref. 17.

Results and Discussion

The high- and low-SiO_2 suites each have $Fe^{3+}/\Sigma Fe$ and $S^{6+}/\Sigma S$ ratios that decrease with decreasing H_2O and S contents (Fig. 1 *A*–*D*), and the glasses within each suite that have the highest S and H_2O concentrations also have the highest proportions of oxidized Fe (Fe^{3+}) and S (S^{6+}). The low-SiO_2 glasses have a narrower range of $Fe^{3+}/\Sigma Fe$ and $S^{6+}/\Sigma S$ ratios and have $Fe^{3+}/\Sigma Fe$ ratios 0.01 to 0.02 units higher than the high-SiO_2 glasses at similar S concentrations (Fig. 1*A*). Despite the subtle differences between the high- and low-SiO_2 glasses, the two suites together define a single overall trend in $Fe^{3+}/\Sigma Fe$ and $S^{6+}/\Sigma S$ space (Fig. 1*E*). Our results demonstrate that degassing of a $S+H_2O+CO_2$ vapor is correlated with reduction of Fe^{3+} to Fe^{2+} and of S^{6+} to S^{2-} (Fig. 1). This result is consistent with recent observations of variable $Fe^{3+}/\Sigma Fe$ ratios in olivine-hosted melt inclusions from Erebus, Kilauea (OIB; shown for comparison with our Mauna Kea data in Fig. 1 *A* and *B*), and Agrigan (arc) volcanoes, although the major element compositions, the S, H_2O, and CO_2 concentrations, and $Fe^{3+}/\Sigma Fe$ ratios in the case of Erebus and Agrigan differ significantly from those studied here, and the Agrigan trend differs from what is observed for other arc glasses (see *SI Appendix*) (10, 16, 17, 28). Our work extends the observation to include direct measurements of the simultaneous reduction of $S^{6+}/\Sigma S$ ratios.

Magmatic fO_2 values relative to the quartz–fayalite–magnetite (QFM) oxygen buffer for each of our samples at 1 atmosphere and 1,200 °C were calculated based on their $Fe^{3+}/\Sigma Fe$ ratios and major element compositions (see *SI Appendix*) (Figs. 2 and 3 *A* and *B* and refs. 8 and 29). Magmatic fO_2 decreases from ~QFM+1.0 in the least degassed samples (i.e., those with highest S and H_2O contents) to ~QFM–0.4 in the most degassed samples (Fig. 3). This ~1.4 orders of magnitude range in fO_2 from the least degassed to the most degassed samples is consistent with inferred and measured fO_2 values for other Hawaiian lavas, based on Fe–Ti oxide oxybarometry (30), gas-mixing experiments (31), gas equilibria (32–34), and XANES measurements of olivine-hosted melt inclusions and matrix glasses from Kilauea (Fig. 2 and refs. 17, 28). A key point is that whole-rock measurements (vertical gray bars, Fig. 2), which represent the final, degassed lava and can be altered rapidly and pervasively at Earth's surface, record highly variable $Fe^{3+}/\Sigma Fe$ ratios that span more than four orders of magnitude fO_2 (Fig. 2), making it difficult to infer from such measurements what the preeruptive fO_2 may have been for Hawaiian magmas. The Fe–Ti oxide record (light gray horizontal bar, Fig. 2), the constraints from gas-mixing experiments (black horizontal bar, Fig. 2), and the $Fe^{3+}/\Sigma Fe$ ratios measured in less degassed melt inclusions (blue vertical bars, Fig. 2) all indicate that the fO_2 of the crystallizing magmas is near QFM+0.2 to QFM+0.8, broadly consistent with the fO_2 of the least degassed magmas from this study.

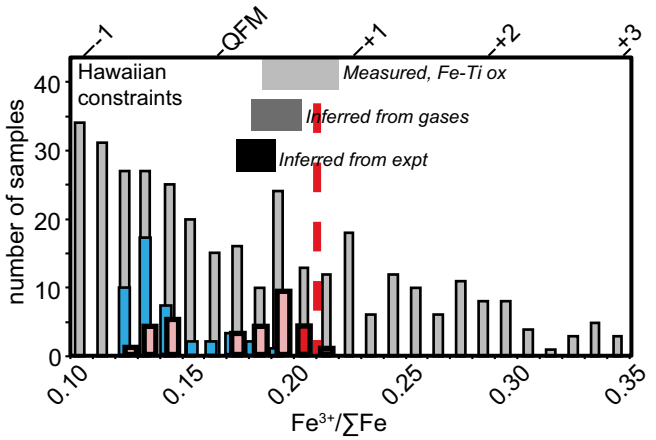

Fig. 2. Histogram comparing $Fe^{3+}/\Sigma Fe$ ratios in 29 HSDP2 glasses (this study, red and pink bars) and 44 glasses from Kilauea volcano (17) (blue bars), all measured using XANES, compared with those in whole rocks measured by wet chemistry (gray bars). Also shown are ranges in fO_2 values at the temperatures relevant for each dataset, relative to QFM (shown as shaded horizontal bars) for Hawaiian volcanism based on analyses of volcanic gases (33, 38) analyses of coexisting Fe–Ti oxides (30), or gas mixing experiments (31). The heavy red vertical dashed line is the average of three undegassed HSDP2 samples. The fO_2 scale on the upper horizontal axis was calculated as in Fig. 1, for a representative MORB composition (42), and should be taken as approximate fO_2 for OIB samples.

We modeled the change in magmatic fO_2 with progressive degassing of a C–O–H–S vapor species using the software package D-Compress, which executes the gas–melt equilibrium model of ref. 35. This thermodynamically based model assumes that, at equilibrium, the chemical potentials of volatile species dissolved in a fluid (i.e., gas)-saturated silicate melt must be equal in the silicate melt and the fluid. Given some constraints on the system (i.e., initial H_2O and CO_2 contents, magmatic fO_2), D-Compress computes the concentration and speciation of C, H, O, and S in coexisting fluid and silicate melt as functions of pressure and temperature, based on experimental calibrations of the solubilities of H_2, H_2O, CO, CO_2, SO_2, H_2S, and S_2 species in silicate melts, and calculations of homogeneous equilibria in the gas phase for the same species. With D-Compress, we calculated redox conditions and coexisting vapor and silicate liquid compositions by progressively decreasing total pressure (at a constant temperature of 1,190 °C; the effect of variable temperature on fO_2 relative to QFM is negligible; see item *i* below) from the assumed starting pressure of 120 bars down to 1 bar, both for fractional (red curves, Fig. 3) and batch (blue curves, Fig. 3) degassing (see *SI Appendix*, *Modeling the Impact of Degassing on Melt* fO2).

Both the fractional and batch models predict a decrease in magmatic fO_2 during the degassing that would accompany depressurization during magma ascent. The fractional model results in a decrease in magmatic fO_2 from QFM+1.1 to QFM−0.2, or about 90% of the observed change in fO_2 observed in the Mauna Kea glasses (Fig. 3). Although the trends are similar for fractional and batch calculations, the models decrease in fO_2 only to QFM (batch) and QFM−0.2 (fractional) when they reach 1 bar (i.e., not quite as much as the fractional degassing model).

The decrease in fO_2 associated with degassing observed in the Mauna Kea glasses is dominated by changes in the speciation of S in the vapor phase. We demonstrate this first by using the same model to simulate degassing of S-free melts in which H_2O or CO_2 was the only dissolved volatile component (H_2O-only case, *SI Appendix*, Fig. S7*A*; CO_2-only case, *SI Appendix*, Fig. S8). We chose melts with much higher volatile contents than observed in the HSDP2 samples of this study to enhance the fO_2 response to degassing. In the H_2O-only and CO_2-only cases (see *SI Appendix*, Fig. S8 for CO_2-only case), the batch-degassing modeling predicts that the fully degassed basaltic melts (i.e., melts decompressed to 1 bar) are, respectively, 0.6 and 0.1 log units higher in fO_2 than the undegassed basaltic magmas that start with 4.5 wt% H_2O or 1,250 ppm CO_2 [note, however, that neither of these extremes results in a change in fO_2 large enough to explain the oxidized nature of arc and back-arc basalts relative to MORB (*SI Appendix*, Fig. S7*A* for H_2O-only case; *SI Appendix*, Fig. S8 for CO_2-only case)]. In the fractional degassing modeling of a H_2O-only vapor produces a basaltic melt at 1 bar total pressure that is 0.7 log units higher in fO_2 than the undegassed basaltic magma, slightly higher than the batch calculation.

In both the batch and fractional degassing scenarios when H_2O is the only volatile component, the increase in melt fO_2 results from the fact that dissolved H_2 is negligible in terrestrial magmas at low pressure (36), but the amount of H_2 in vapor coexisting with hydrous melt is not. Consequently, when dissolved H_2O is transferred from the melt into the vapor, H_2 is generated in the vapor by disproportionation of a fraction of the H_2O. This disproportionation must likewise generate an equal amount of O_2, but, since, at these fO_2 levels, fH_2/fO_2 in the vapor is much greater than 1, the excess oxygen generated by disproportion of H_2O is partitioned into the coexisting melt, resulting in increases in fO_2, and $Fe^{3+}/\Sigma Fe$ and $S^{6+}/\Sigma S$ ratios in the melt. In C-bearing systems, the assumed negligible amount of CO dissolved in the melt but the nonnegligible CO content of the vapor leads to the same effect when CO_2 is transferred from the melt in the vapor (see *SI Appendix*, Fig. S8).

We also simulated the degassing of basaltic melt in which S-bearing species are the dominant volatile components dissolved in the melt. The model basaltic melt contains 6,000 ppm S, no C, and 128 ppm total H (the amount of H necessary to make H_2S and 0.1 wt% H_2O). In this S-dominant case, the model predicts that,

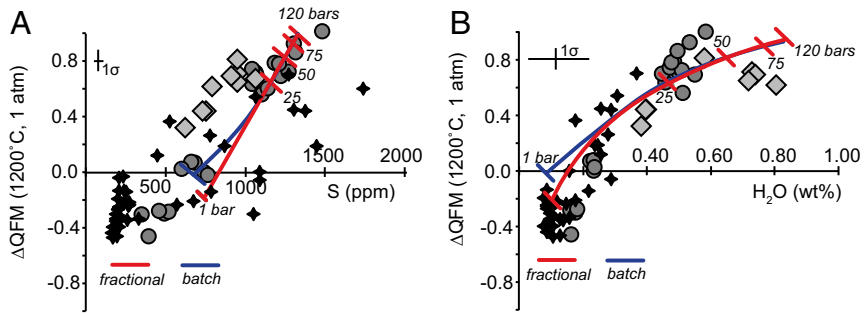

Fig. 3. (*A*) The fO_2 values (relative to QFM) for each of the HSDP glasses (calculated as in Fig. 1) vs. S concentration of the glass (24). Also shown are the results of fractional (red curve) and batch (blue curve) degassing calculations based on the D-Compress software from ref. 35. Tick marks represent increments of decompression from 120 bars to 1 bar total pressure. Symbols are as in Fig. 1. (*B*) Same as *A*, except fO_2 is shown vs. H_2O content of the glass.

for batch degassing, on decompression to 1 bar, the melt is 1.3 log units lower in fO_2 than the undegassed melt (*SI Appendix*, Fig. S7*B*); the fO_2 decreases by more than 1.5 log units for fractional degassing. In systems in which S is the dominant volatile element, the change in fO_2 during degassing is more complex than for CO_2- and H_2O-dominant systems because S is present both as sulfide and sulfate in the melt, and in multiple oxidation states (i.e., S_2, H_2S, and SO_2) in the vapor as well. We nevertheless are able to infer that the decrease in fO_2 upon degassing for the modeled S-dominant basaltic melt (*SI Appendix*, Fig. S7*B*) is dominated by the conversion of sulfide dissolved in the melt to SO_2 in the vapor. That is, as suggested by many previous authors (e.g., refs. 6, 10, 16, 17, 28, 30, and 37), degassing reactions such as $3Fe_2O_3$(melt) + FeS(melt) = 7FeO(melt) + SO_2(vapor) lead to a decrease in the $Fe^{3+}/\Sigma Fe$ ratios, to a decrease in $S^{6+}/\Sigma S$ ratios of the residual S dissolved in the melt (i.e., Fig. 1 *A*, *C*, and *E*), and thus to a decrease in the fO_2 of the system.

In a system containing H_2O, S, ± CO_2 at the fO_2 levels appropriate to Hawaiian magmas, the tendency of H_2O and CO_2 degassing to increase the fO_2 is overwhelmed by the tendency to decrease the fO_2 due to degassing of S-bearing species. For Hawaiian magmas, it is known that CO_2 is the dominant degassing volatile component until pressures of ∼100 bars (e.g., ref. 38), at which point H_2O and S come out nearly simultaneously. The degassing of dominantly CO_2 at pressures higher than that at which H_2O and S begin to transfer from melt to vapor in significant quantities increases fO_2 slightly, but further decreases in pressure that result in simultaneous degassing of H_2O and S-bearing species at low pressure lead to significant decrease in fO_2 (*SI Appendix*, Fig. S8). We emphasize, however, that the effects of degassing on fO_2 will depend on the sequence of loss of the volatile species with decreasing pressure, which in turn depends on both the solubilities of volatile species and on the initial abundances of volatile components in the undegassed magma.

The least degassed Mauna Kea glasses record an fO_2 that is approximately one order of magnitude higher than MORB glasses at similar MgO contents; i.e., corresponding to $Fe^{3+}/\Sigma Fe$ of ∼0.22 for the HSDP2 samples, compared with $Fe^{3+}/\Sigma Fe$ of ∼0.16 for MORB (*SI Appendix*, Fig. S10). This result is broadly similar to results from XANES measurements of matrix glasses and melt incusions from Kilauea volcano (17, 28), although the highest fO_2 values from the Mauna Kea glasses (QFM+1.0; this study) are higher than those from Kilauea (QFM+0.7; refs. 17 and 28). However, the $Fe^{3+}/\Sigma Fe$ ratios and inferred fO_2 values of degassed Mauna Kea glasses overlap with those of average undegassed MORB, and, if the reducing effects of low-pressure degassing were not taken into account, it might be concluded that parental magmas and mantle sources at Mauna Kea had fO_2 values similar to those of MORB parental magmas and their mantle sources. However, the appropriate comparison is between the least-degassed samples from Mauna Kea and the MORB glasses. Although this comparison indicates that undegassed Mauna Kea magmas were, on eruption, more oxidized than MORB, caution must be exercised in generalizing this statement to their parental magmas and to their mantle source regions.

The mantle sources of Hawaiian magmas are at higher pressures and temperatures than MORB magmas (e.g., ref. 39 and references therein), and corrections must be made to the fO_2 values based on measurements of fractionated, lower-pressure and -temperature glasses to determine the fO_2 values that prevailed in their mantle sources.

i) The relative change in fO_2 of silicate liquids and the fO_2 of the QFM oxygen buffer at constant pressure and increasing temperature is small [<0.005 log unit decrease from 1,200 °C to 1,400 °C at 1 GPa, and <0.02 log unit decrease in the same temperature range at 3 GPa (8, 29)], so the effect of the temperature differences between MORBs [1,400 °C to 1,525 °C (39)] and undegassed Hawaiian magmas [∼1,725 °C (39)] on inferences about their source fO_2 relative to the QFM oxygen buffer can be neglected.

ii) In contrast, the relative change in fO_2 of silicate liquids and the fO_2 of the QFM oxygen buffer at constant temperature and increasing pressure is nonnegligible: The fO_2 of a typical basaltic silicate liquid increases by 0.39 log units relative to QFM when pressure increases from 1 bar to 3 GPa at 1,300 °C and by 0.36 log units relative to QFM over the same pressure interval at 1,450 °C (8, 29). Thus, assuming a typical average pressure of ∼1.0 GPa for MORB melt generation (e.g., ref. 40) and ∼3 GPa for Hawaiian melt generation (e.g., ref. 41 and references therein), the approximately one order of magnitude higher fO_2 (relative to the QFM buffer at 1 atmosphere) of the undegassed HSDP2 glasses relative to MORB glasses increases to ∼1.14 orders of magnitude (relative to the QFM buffer at the pressure of melt generation) difference in their sources after correcting for pressure alone.

iii) Considerable (and different amounts of) olivine fractionation occurred between the generation of primary melts in their mantle source regions and the eruption of the melts from which MORB and Hawaiian glasses were quenched. Assuming that crystallization occurs at a constant total oxygen content for the system, the effect of olivine crystallization is to increase $Fe^{3+}/\Sigma Fe$ and increasing fO_2 with progressive fractionation, potentially overprinting differences that may have existed between the unfractionated primary melts equilibrated with their residual mantle sources. Mauna Kea primary liquids are thought to have as much as 18 wt% to 20 wt% MgO, assuming they equilibrated with Fo_{91} olivines in their sources (41), whereas MORB primary magmas are thought to have only 12 wt% to 14 wt% MgO, assuming they equilibrated with Fo_{90} olivines in their sources (e.g., ref. 42; see *SI Appendix*). If this is correct, then primary Mauna Kea liquids fractionated a larger amount of olivine than MORB magmas (44% olivine removed for Mauna Kea, compared with 23% for MORB) to reach 7 wt% MgO. We calculated the $Fe^{3+}/\Sigma Fe$ ratios and fO_2 of primary mantle melts for MORB and Mauna Kea by taking an undegassed composition from each setting and adding the equilibrium composition olivine back to the melt in 0.1% increments, treating Fe^{2+} and Fe^{3+} as conservative elements (see *SI Appendix*). This can account for 0.5 ± 0.1 log units (the uncertainty estimate accounts for the range of primary melt MgO contents described above) of the observed difference in fO_2 between undegassed Mauna Kea and MORB melts. When combined with the temperature and pressure effect on silicate melts in items *i* and *ii*, this results in a calculated difference in fO_2 between Mauna Kea and MORB sources of 0.66 ± 0.1 log units, compared with the ∼1.16 log unit difference between the fO_2 values of the erupted, highly fractionated melts preserved as glasses.

iv) It has been suggested that lower temperatures of melting can generate melts with higher abundances of Fe^{3+} than melts produced during normal MORB melting and that it might be difficult to distinguish unambiguously melts of an intrinsically oxidized source from those of a lower-temperature source because both would have relatively high $Fe^{3+}/\Sigma Fe$ ratios (43). Although we have not tried to quantify this effect, if the reverse temperature effect were true (i.e., that higher temperatures lead to melts with lower Fe^{3+} abundances; e.g., ref. 15), the fact that the Hawaiian plume is generally thought to have an elevated mantle potential temperature of ∼1,725 °C compared with 1,400 °C to 1,525 °C for MORB sources (39) suggests that unmelted Hawaiian sources have even higher fO_2 relative to MORB sources than suggested by direct comparison of differences in $Fe^{3+}/\Sigma Fe$ ratios between the melts of these sources. To the degree that this temperature effect is important, it would suggest that the residual sources of the Hawaiian melts studied

here are more than ~0.66 log units more oxidized relative to QFM than MORB primary magmas; i.e., the ~0.66 log unit higher fO_2 of Hawaiian primary magmas relative to MORB magmas would be a lower limit to the differences in the fO_2 values of their source regions before melting.

After considering these petrogenetic factors, we conclude that the difference in fO_2 between the sources of Mauna Kea magmas and MORBs, while less than that suggested by the "raw" $Fe^{3+}/\Sigma Fe$ ratios of undegassed Mauna Kea and MORB glasses, is still significant at $\gtrsim 0.6 \pm 0.1$ log units relative to QFM. The higher fO_2 values of undegassed Hawaiian magmas relative to MORBs in turn reflect differences in the fO_2 values of the Hawaiian plume relative to MORB sources. This suggests that differences in fO_2 in the modern upper mantle are not restricted to the ~1.3 orders of magnitude difference between the subarc mantle wedge (generally attributed to recycling of oxidized sediments and crust by subduction) and the mantle beneath ridges (likely representative of most of the upper mantle) summarized in the Introduction. If, as is widely thought (18, 25, 44), the sources of OIBs, including Hawaii, contain near-surface material recycled by plate tectonics into the deep mantle that is then returned to the surface in the form of ocean island volcanism, the higher fO_2 value relative to the QFM buffer inferred for the mantle sources of the Mauna Kea samples relative to the sources of MORBs could simply reflect that the recycled plume component(s) are more oxidized than the average mantle. This hypothesis is also consistent with observations that Mauna Kea submarine glasses from the studied intervals in the HSDP2 core have relatively radiogenic Sr (0.7035 to 0.7037) and nonradiogenic Nd isotopic compositions [0.51216 to 0.51219 (25)], two characteristics consistent with the presence of recycled components in the Hawaiian plume: either recycled sediment and/or oceanic crust (e.g., refs. 25, 45, and 46). If we approximate the primary melt of Mauna Kea magmas as a simple mixture between a primary melt of garnet-bearing lherzolite, with 5.6 wt% FeO* (3 GPa melt composition from ref. 47) and 1.0 wt% Fe_2O_3 [the Fe_2O_3 content corresponding to a melt at 3GPa, 1,450 °C, and QFM (8)], and average altered oceanic crust, with 5 wt% FeO* and 1.97 wt% Fe_2O_3 (13), it suggests that ~20% of the sources of Mauna Kea primary melts (with $Fe^{3+}/\Sigma Fe$ ~0.142; see *SI Appendix*) is derived from altered oceanic crust in the Hawaiian plume. This is similar to the high end of the range of other estimates for the amount of recycled material present in the Hawaiian plume [4 to 20% (45, 48, 49)] based on the major and trace element and isotopic compositions of Hawaiian lavas.

Using our results as a starting point, we now consider the influence of gas evolved during degassing of basaltic magmas on the oxidation state of the atmosphere. Volcanic gases are an important input to the inventory of H-, S-, and C-bearing molecules in the atmosphere, oceans, and crust (e.g., ref. 50), and it has been hypothesized that a change in the oxidation state of volcanic gases played a role in the "Great Oxidation Event" at ~2.3 Ga (e.g., refs. 21 and 51–55). The general idea is that, before the rise of atmospheric O_2, volcanic gas compositions were, overall, more reducing compared with their Proterozoic and Phanerozoic counterparts, leading to increased sinks for atmospheric O_2 that would have limited the accumulation of O_2 produced by oxygenic photosynthesis (i.e., volcanic gases had a value of $f > 1$ according to Holland's criterion, Eq. **1** below). Then, a change in magmatic fO_2 (22) or volcanic degassing conditions (21, 53) led to a change in the composition of volcanic gases added to the atmosphere that resulted in their being more oxidizing, such that volcanic gases no longer contained enough reducing power to titrate the photosynthetic production of O_2, which thereafter began to accumulate in the atmosphere [i.e., volcanic gases had a value of $f < 1$ (54)]. This capacity for volcanic gases to react with and remove atmospheric O_2 has been referred to as the "reducing power," and is characterized using Holland's criterion based on the parameter, f (54) (m_i is the mole fraction of species i in a volcanic gas), defined as

$$f = \frac{m_{H2} + 0.6\, m_{CO} - 0.4\, m_{CO2} + 3\, m_{H2S}}{3.5\, (m_{SO2} + m_{H2S})} + \frac{1}{3.5}. \quad [1]$$

We calculated the f value for the incremental gas composition in equilibrium with the decompressing magma that is provided from the modeled degassing trajectory of Mauna Kea lavas shown in Fig. 3. The value of f at all pressure increments is ~0.5, does not vary significantly upon decompression from 120 bars to 1 bar, and is consistent with an atmosphere that allows for the accumulation of photosynthetically produced O_2. Thus, to the degree that degassing of Hawaiian magmas can represent degassing of Archean magmas, they would not have been sufficiently reducing to preclude the accumulation of O_2 in the ancient atmosphere if oxygenic photosynthesis was prevalent at that time. We note that the relative constancy from our modeling of f during decompression is inconsistent with suggestions that a systematic decrease in the pressure of degassing from 100 bars to 1 bar (i.e., a result of the production of subaerial continental crust, thus enabling magmas to degas directly to the atmosphere) could have led to atmospheric oxygenation (i.e., by reducing f from a value of >1 to <1). These suggestions were based on the increase in SO_2/H_2S ratio of volcanic gases with decreasing pressure, and the assumption that, at high pressure, emissions of SO_2 are negligible. However, the SO_2/H_2S ratio of volcanic gases at these pressures can be ~0.5 to 1.0, indicating that SO_2 emissions at these pressures cannot be assumed to be negligible. Moreover, there are significant changes in C abundance and speciation in the gas phase over this pressure range that must be considered simultaneously with changes in sulfur speciation. Model degassing trajectories for modern MORB-like and arc-like magmas (*SI Appendix*, Fig. 11) demonstrate that the f value of these gases can be low at high pressures when CO_2 dominates the gas composition (at 1,000 bar, $f = -16$ for MORB and $f = -10$ for arc magmas) and increase dramatically as the total C content of the gas decreases and the proportion of CO_2 to CO decreases (at 10 bar, $f = -5$ for MORB and $f = -3$ for arc magmas). Nevertheless, the degassing scenarios examined here have $f < 1$ for the entire degassing trajectory, and they do not suggest that any reasonable changes in volatile contents or pressures of degassing would lead to the production of volcanic gases with $f > 1$. Thus, given their fO_2 values, degassing of any of the most abundant igneous rocks on Earth today would, regardless of the pressure of degassing or their volatile contents, support oxygen accumulation in the atmosphere. Only if we decrease the fO_2 of the degassing magma in our calculations to QFM−2.3 do the released incremental volcanic gases have f > ~1 (solid gray line, *SI Appendix*, Fig. S11*C*). Consequently, we take this to be the upper limit of fO_2 for degassing magmas that would have been capable of diminishing atmospheric O_2 concentrations. These results are broadly similar to calculations presented by ref. 55, except that they place the upper limit of fO_2 for degassing magmas capable of diminishing atmospheric O_2 concentrations somewhat higher, near QFM−1.8. In that work, average volcanic gas-phase chemistry was estimated from present-day measurements of volcanic gas emissions, which may contribute to the difference in upper limits between our study and that of ref. 55.

Our degassing calculations suggest that changes in the average degassing pressure of the most abundant modern basaltic magma types (i.e., the calculations on Mauna Kea lavas as representative of OIBs and on representative MORB and arc compositions summarized in *SI Appendix*, Fig. S11) could not have strongly influenced the oxygen-poor conditions at Earth's surface before ~2.3 Ga. For volcanic processes to have been responsible for inhibiting the rise of oxygen in the Archean, magmas would have to have been, on average, more reduced than modern MORB magmas by more than two orders of magnitude (*SI Appendix*, Fig. S11).

Vanadium contents in olivines in Archean komatiites suggest that magmatic fO_2 in Archean komatiites were between QFM−1 and QFM+2 (56), which is outside of the range of fO_2 levels required to prevent oxygenation of the atmosphere, based on our calculations, as well as those presented by ref. 55. If these trace metal constraints accurately describe the redox state of average Archean magmas, then volcanic gases from Archean magmas would also have been unable to limit oxygenation of the atmosphere if photosynthetic microbes were present at that time. We conclude that, if volcanic processes are required to play a major role in inhibiting the rise of oxygen in the Archean, either photosynthetic microbes were not present or Archean basalts were significantly more reducing than modern magmas or than current evidence suggests for Archean basalts.

ACKNOWLEDGMENTS. We thank A. Lanzirotti and M. Newville for assistance in beamline operations at Advanced Photon Source Argonne National Laboratory (APS ANL). We thank Woody Fisher and Oliver Shorttle for commenting on early versions of this manuscript. This research used resources of APS, a US Department of Energy (DOE) Office of Science user facility operated for the DOE Office of Science by ANL under Contract DE-AC02-06CH11357. We thank the Department of Mineral Sciences, Smithsonian Institute, for access to sample NMNH 117393.

1. Osborn EF (1959) Role of oxygen pressure in the crystallization and differentiation of basaltic magma. *Am J Sci* 257:609–647.
2. Wood BJ, Bryndzia LT, Johnson KE (1990) Mantle oxidation state and its relationship to tectonic environment and fluid speciation. *Science* 248:337–345.
3. Carmichael ISE (1991) The redox states of basic and silicic magmas: S reflection of their source regions? *Contrib Min Pet* 106:129–141.
4. Wallace PJ, Carmichael ISE (1991) Sulfur in basaltic magmas. *Geochim Cosmochim Acta* 56:1863–1874.
5. Nilsson K, Peach CL (1993) Sulfur speciation, oxidation state, and sulfur concentration in backarc magmas. *Geochim Cosmochim Acta* 57:3807–3813.
6. Metrich N, Berry A, O'Neill H, Susini J (2009) The oxidation state of sulfur in synthetic and natural glasses determined by X-ray absorption spectroscopy. *Geochim Cosmochim Acta* 73:2382–2399.
7. Brounce M, Kelley KA, Cottrell E (2014) $Fe^{3+}/\Sigma Fe$ variations in Mariana Arc basalts and primary fO_2 of the mantle wedge. *J Pet* 55:2513–2536.
8. Kress VC, Carmichael ISE (1991) The compressibility of silicate liquids containing Fe_2O_3 and the effect of composition, temperature, oxygen fugacity and pressure on their redox states. *Contrib Min Petl* 108:82–92.
9. Jugo PJ, Wilke M, Botcharnikov RE (2010) Sulfur K-edge XANES analysis of natural and synthetic basaltic glasses: Implications for S speciation and S content as function of oxygen fugacity. *Geochim Cosmochim Acta* 74:5926–5938.
10. Kelley KA, Cottrell E (2012) The influence of magmatic differentiation on the oxidation state of Fe in a basaltic arc magma. *Earth Planet Sci Lett* 329-330:109–121.
11. Brounce M, Kelley KA, Cottrell E, Reagan MK (2015) Temporal evolution of mantle wedge oxygen fugacity during subduction initiation. *Geology* 43:775–778.
12. Parkinson IJ, Arculus RJ (1999) The redox state of subduction zones: Insights from arc-peridotites. *Chem Geol* 160:409–424.
13. Lecuyer C, Ricard Y (1999) Long-term fluxes and budget of ferric iron: Implication for the redox states of the Earth's mantle and atmosphere. *Earth Planet Sci Lett* 165:197–211.
14. Rhodes JM, Vollinger MJ (2005) Ferric/ferrous ratios in 1984 Mauna Loa lavas: A contribution to understanding the oxidation state of Hawaiian magmas. *Contrib Min Pet* 149:666–674.
15. Shorttle O, et al. (2015) Fe-XANES analyses of Reykjanes Ridge basalts: Implications for oceanic crust's role in the solid Earth oxygen cycle. *Earth Planet Sci Lett* 427:272–285.
16. Moussallam Y, et al. (2014) Tracking the changing oxidation state of Erebus magmas, from mantle to surface, driven by magma ascent and degassing. *Earth Planet Sci Lett* 393:200–209.
17. Moussallam Y, et al. (2016) The impact of degassing on the oxidation state of basaltic magmas: A case study of Kilauea volcano. *Earth Planet Sci Lett* 450:317–325.
18. Hofmann AW, White WM (1982) Mantle plumes from ancient oceanic crust. *Earth Planet Sci Lett* 57:421–436.
19. Holloway J (2004) Redox reactions in seafloor basalts: Possible insights into silicic hydrothermal systems. *Chem Geol* 210:225–230.
20. Mathez EA, Delaney JR (1981) The nature and distribution of carbon in submarine basalts and peridotite nodules. *Earth Planet Sci Lett* 56:217–232.
21. Gaillard F, Scaillet B, Arndt NT (2011) Atmospheric oxygenation caused by a change in volcanic degassing pressure. *Nature* 478:229–232.
22. Kump LR, Kasting JF, Barley ME (2001) Rise of atmospheric oxygen and the "upside-down" Archean mantle. *Geochem Geophys Geosyst* 2:1025.
23. Stolper EM, DePaolo DJ, Thomas DM (2009) Deep drilling into a mantle plume volcano: The Hawai'i Scientific Drilling Project. *Sci Drill* 7:4–14.
24. Seaman C, et al. (2004) Volatiles in glasses from the HSDP2 drill core. *Geochem Geophys Geosyst* 5:Q09G16.
25. Bryce JG, DePaolo DJ, Lassiter JC (2005) Geochemical structure of the Hawaiian plume: Sr, Nd, and Os isotopes in the 2.8 km HSDP-2 section of Mauna Kea volcano. *Geochem Geophys Geosyst* 6:Q09G18.
26. Stolper E, Sherman S, Garcia M, Baker M, Seaman C (2004) Glass in the submarine section of the HSDP2 drill core, Hilo, Hawaii. *Geochem Geophys Geosyst* 5:Q07G15.
27. Rhodes JM, Vollinger MJ (2004) Composition of basaltic lavas sampled by phase-2 of the Hawaii Scientific Drilling Project: Geochemical stratigraphy and magma types. *Geochem Geophys Geosyst* 5:Q03G13.
28. Helz RT, Cottrell E, Brounce MN, Kelley KA (2017) Olivine-melt relationships and syneruptive redox variations in the 1959 eruption of Kilauea Volcano as revealed by XANES. *J Volcanol Geotherm Res* 333-334:1–14.
29. Frost BR (1991) Introduction to oxygen fugacity and its petrologic importance. *Rev Mineral Geochem* 25:1–9.
30. Anderson AT, Wright TL (1972) Phenocrysts and glass inclusions and their bearing on oxidation and mixing of basaltic magmas, Kilauea volcano, Hawaii. *Am Mineral* 57:188–216.
31. Fudali RF (1965) Oxygen fugacities of basaltic and andesitic magmas. *Geochim Cosmochim Acta* 29:1063–1075.
32. Heald EF, Naughton JJ, Barnes ILJ (1963) The chemistry of volcanic gases 2: Use of equilibrium calculations in the interpretation of volcanic gas samples. *J Geophys Res* 68:545–557.
33. Sato M, Wright TL (1966) Oxygen fugacities directly measured in magmatic gases. *Science* 153:1103–1105.
34. Gerlach TM (1993) Oxygen buffering of Kilauea volcanic gases and the oxygen fugacity of Kilauea basalt. *Geochim Cosmochim Acta* 57:795–814.
35. Burgisser A, Alletti M, Scaillet B (2015) Simulating the behavior of volatiles belonging to the C–O–H–S system in silicate melts under magmatic conditions with the software D-Compress. *Comput Geosci* 79:1–14.
36. Hirschmann MM, Withers AC, Ardia P, Foley NT (2012) Solubility of molecular hydrogen in silicate melts and consequences for volatile evolution of terrestrial planets. *Earth Planet Sci Lett* 345:38–48.
37. Carmichael ISE, Ghiorso MS (1986) Oxidation-reduction relations in basic magma: A case of homogeneous equilibria. *Earth Planet Sci Lett* 78:200–210.
38. Gerlach TM, Graeber EJ (1985) Volatile budget of Kilauea volcano. *Nature* 313: 273–277.
39. Putirka KD, Perfit M, Ryerson FJ, Jackson MG (2007) Ambient and excess mantle temperatures, olivine thermometry, and active vs passive upwelling. *Chem Geol* 241: 177–206.
40. Langmuir CH, Klein EM, Plank T (1992) Petrological systematics of mid-ocean ridge basalts: Constraints on melt generation beneath ocean ridges. *Geophys Monogr* 71:183–280.
41. Herzberg C (2010) Identification of source lithology in the Hawaiian and Canary Islands: Implications for origins. *J Petrol* 52:113–146.
42. Cottrell E, Kelley KA (2011) The oxidation state of Fe in MORB glasses and the oxygen fugacity of the upper mantle. *Earth Planet Sci Lett* 305:270–282.
43. Gaetani G (2016) The behavior of Fe3+/ΣFe during partial melting of spinel lherzolite. *Geochim Cosmochim Acta* 185:64–77.
44. White WM (2010) Oceanic island basalts and mantle plumes: The geochemical perspective. *Annu Rev Earth Planet Sci* 38:133–160.
45. Eiler JM, Farley KA, Valley JW, Hoffman AW, Stolper EM (1996) Oxygen isotope constraints on the sources of Hawaiian volcanism. *Earth Planet Sci Lett* 144:453–468.
46. Lassiter JC, DePaolo DJ, Tatsumoto M (1996) Isotopic evolution of Mauna Kea volcano: Results from the initial phase of the Hawaii Scientific Drilling Project. *J Geophys Res* 101:11769–11780.
47. Walter MJ (1998) Melting of garnet peridotite and the origin of komatiite and depleted lithosphere. *J Petrol* 39:29–60.
48. Hauri EH, Lassiter JC, DePaolo DJ (1996) Osmium isotope systematics of drilled lavas from Mauna Loa, Hawaii. *J Geophys Res Solid Earth* 101:11793–11806.
49. Sobolev AV, et al. (2007) The amount of recycled crust in sources of mantle-derived melts. *Science* 316:412–417.
50. Halmer MM, Schmincke HU, Graf HF (2002) The annual volcanic gas input into the atmosphere, in particular into the stratosphere: A global data set for the past 100 years. *J Volcanol Geotherm Res* 115:511–528.
51. Holland HD (1984) *The Chemical Evolution of the Atmosphere and Oceans* (Princeton Univ Press, Princeton).
52. Kasting JF, Eggler DH, Raeburn SP (1993) Mantle redox evolution and the oxidation state of the Archean atmosphere. *J Geol* 101:245–257.
53. Kump LR, Barley ME (2007) Increased subaerial volcanism and the rise of atmospheric oxygen 2.5 billion years ago. *Nature* 448:1033–1036.
54. Holland HD (2002) Volcanic gases, black smokers, and the Great Oxidation Event. *Geochim Cosmochim Acta* 66:3811–3826.
55. Li ZXA, Lee C-TA (2004) The constancy of upper mantle fO_2 through time inferred from V/Sc ratios in basalts. *Earth Planet Sci Lett* 228:483–493.
56. Canil D (2002) Vanadium in peridotites, mantle redox and tectonic environments: Archean to present. *Earth Planet Sci Lett* 195:75–90.